ChemBioChem

Research Article
doi.org/10.1002/cbic.202300498

Chemistry Europe
European Chemical Societies Publishing

www.chembiochem.org

Synthesis and Evaluation of Cereblon-Recruiting HaloPROTACs

Britton K. Ody[+],[a] Jing Zhang[+],[a] Sydney E. Nelson[+],[b] Yayun Xie[+],[a] Ruochuan Liu,[a] Cayden J. Dodd,[b] Savannah E. Jacobs,[a] Savannah L. Whitzel,[b] Leighan A. Williams,[b] Samer Gozem,[c] Mark Turlington,*[b] and Jun Yin*[a]

Target validation is key to the development of protein degrading molecules such as proteolysis-targeting chimeras (PROTACs) to identify cellular proteins amenable for induced degradation by the ubiquitin-proteasome system (UPS). Previously the HaloPROTAC system was developed to screen targets of PROTACs by linking the chlorohexyl group with the ligands of E3 ubiquitin ligases VHL and cIAP1 to recruit target proteins fused to the HaloTag for E3-catalyzed ubiquitination. Reported here are HaloPROTACs that engage the cereblon (CRBN) E3 to ubiquitinate and degrade HaloTagged proteins. A focused library of CRBN-pairing HaloPROTACs was synthesized and screened to identify efficient degraders of EGFP-HaloTag fusion with higher activities than VHL-engaging HaloPROTACs at sub-micromolar concentrations of the compound. The CRBN-engaging HaloPROTACs broadens the scope of the E3 ubiquitin ligases that can be utilized to screen suitable targets for induced protein degradation in the cell.

The development of proteolysis-targeting chimeras (PROTAC) confers a new modality of drug-like small molecules that have unique activities in inducing protein degradation by the ubiquitin-proteasome system (UPS) in the cell.[1] A typical PROTAC follows a heterobifunctional design in which ligands specific for an E3 ubiquitin ligase and a target protein are tethered through linkers of variable lengths to recruit target proteins to the E3 for proximity-based ubiquitination to signal their degradation by the proteasome.[2] While ligands of E3s have been developed to assemble PROTACs partnering with various E3s such as Cullin 2 (Cul2)-von Hippel-Lindau protein (VHL), Cullin 4 (Cul4)-cereblon (CRBN), and cellular inhibitor of apoptosis protein 1 (cIAP1),[1a,b,3] much effort is devoted to screening ligands against cellular targets to enable their degradation by the PROTACs. Before the commitment to the ligand discovery effort for specific cellular targets, it is desirable to screen a panel of cellular proteins to identify the ones that can be removed by UPS with high efficiency and, upon their removal, can generate the desired cellular response for therapeutical exploration. Methods for target identification and validation have been developed to tag the proteins of interest with a genetically encoded tag so that PROTACs functionalized with a tag-specific ligand can be used to recruit the target proteins to the E3 for ubiquitination, and subsequently, the dynamics of the target degradation and cellular response can be evaluated. So far, a variety of tags have been developed to assay protein degradation, including HaloTag,[4] a repurposed dehalogenase, the degradation tag (dTAG) based on variants of FK506-binding protein 12 (FKBP12),[5] BromoTag originated from the BRD4 bromodomain,[6] and the NanoLuc tag, an engineered luciferase.[7]

HaloTag is a genetically modified bacterial dehalogenase that forms covalent bonds with ligands functionalized with terminal chlorohexyl moieties.[8] It is a popular choice for tagging cellular targets to validate their degradation by the UPS because the chlorohexyl group can be readily attached to E3 ligands through a linker to generate the bivalent HaloPROTAC that can trigger the ubiquitination and degradation of the tagged proteins (Figure 1). So far, HaloPROTACs engaging VHL and cIAP E3s have been developed, while the HaloPROTAC recruiting CRBN for induced protein degradation is missing.[4a,d,9]

As most currently developed PROTACs utilize the VHL and CRBN ubiquitin ligases, we reasoned that the development of CRBN-recruiting HaloPROTACs would expand the versatility of this class of chemical probes as it has been shown that different E3 ligase ligands produce distinct degradation profiles.[5a] Furthermore, various cell and tissue types have substantially different expression levels of the E3s.[10] Thus, diversifying the E3-HaloPROTAC pairs could broaden the use of HaloTag-based platform for target validation in a larger bandwidth of cell types. Also advantageous in our minds, ligands that target CRBN (e.g., pomalidomide, thalidomide) are structurally simpler than the VHL and cIAP1 ligands, and thus chorohexyl-functionalized CRBN ligands present the opportunity to develop

[a] B. K. Ody,[+] J. Zhang,[+] Y. Xie,[+] Dr. R. Liu, S. E. Jacobs, Prof. Dr. J. Yin
Department of Chemistry
Center for Diagnostics and Therapeutics
Georgia State University
Atlanta, GA 30303 (USA)
E-mail: junyin@gsu.edu

[b] S. E. Nelson,[+] C. J. Dodd, S. L. Whitzel, L. A. Williams, Prof. Dr. M. Turlington
Department of Chemistry and Biochemistry
Berry College
Mount Berry, GA 30149 (USA)
E-mail: mturlington@Berry.edu

[c] Prof. Dr. S. Gozem
Department of Chemistry, Georgia State University
Atlanta, GA, 30303 (USA)

[+] These authors contributed equally to this work.

Supporting information for this article is available on the WWW under https://doi.org/10.1002/cbic.202300498

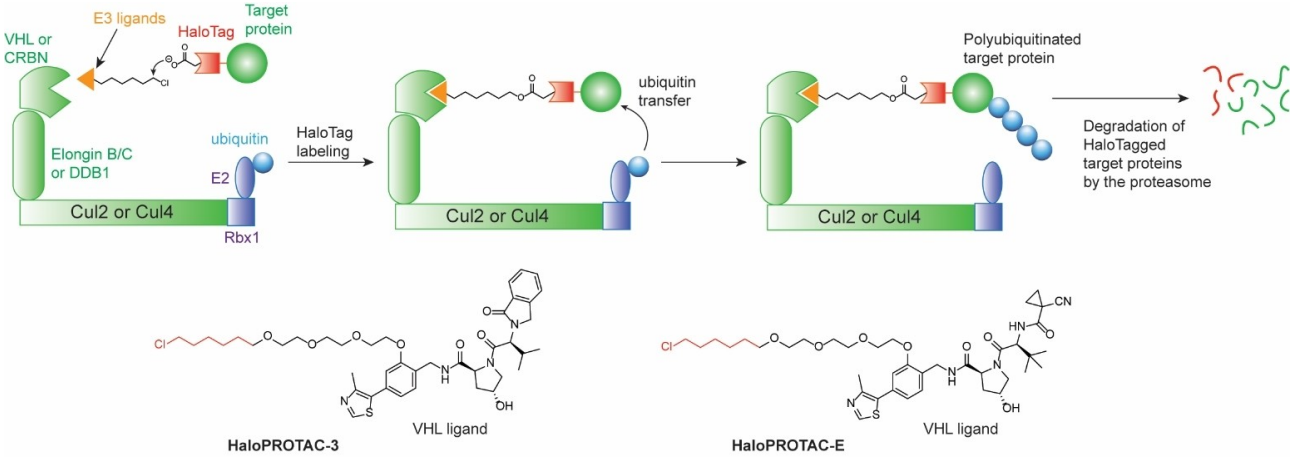

Figure 1. The mechanism of actions of bifunctional HalPROTAC ligands that pair with VHL or CRBN E3s to induce the ubiquitination and degradation of target proteins fused with a HaloTag. The VHL E3 complex utilize Cullin 2 (Cul2) as a scaffold that binds to the VHL through the bridging of Elongin B and C at one end and E2 through the bridging of Rbx1 at the other end. PROTAC ligands pairing with VHL such as HaloPROTAC-3 and HaloPROTAC-E would bind to VHL and covalently react with the HaloTag fused to the target proteins to recruit the targets to the E3 complex to induce their ubiquitination by proximity.[1] Polyubiquitinated target proteins would then be recognized by proteasome for degradation. This study developed a HaloPROTAC that is equipped with a CRBN ligand to recruit HaloTagged target proteins to the CRBN E3 complex consisting of Cullin 4 (Cul4), DDB1, and CRBN to induce their ubiquitination and degradation.

HaloPROTACs with streamlined synthetic routes and lower molecular weights to improve their pharmaceutical properties. Consequently, we set out to develop CRBN-recruiting HaloPROTACs to diversify the E3 pool engaged by HaloPROTACs in order to broaden the scope of the HaloTag-based target validation method. Herein we report the development of HaloPROTACs capable of recruiting the CRBN E3 ligase to induce protein degradation.

For our CRBN-recruiting HaloPROTAC design, we attached linkers of variable lengths with a terminal chlorohexyl moiety to the CRBN ligand pomalidomide at alternative positions and screened the activities of the HaloPROTAC molecules in inducing the degradation of EGFP fused to HaloTag2. Previously the EGFP-Halotag2 fusion has been used to validate the activity of hydrophobic tags for induced protein degradation.[4c,11] The reported design of VHL-recruiting HaloPROTAC-3 and HaloPROTAC-E demonstrated that degradation efficiency depended both on the point of linker attachment and linker length.[4a,d] Accordingly, in designing CRBN-recruiting HaloPROTACs, we attached linkers at either the 4- or 5-positions of the CRBN ligand as shown in Scheme 1. We also followed the Crews strategy of synthesizing longer linkers (15–21 atoms in length) since shorter linkers (6–12 atoms) were ineffective for VHL-pairing HaloPROTACs.[4d]

The synthesis of our CRBN-recruiting HaloPROTACs (Scheme 1) began with the addition of 1-chloro-6-iodohexane to ethylene glycols of various lengths to produce **1a**–**1c**. These were then reacted with *tert*-butyl bromoacetate to construct *tert*-butyl ester-containing linkers **2a**–**2c**. Ester hydrolysis using formic acid, followed by acid chloride formation using oxalyl chloride and catalytic DMF, produced acid chlorides **3a**–**3c**, which were immediately coupled with commercially available pomalidomide (4-amino substitution) or the 5-amino substituted analog prepared via Brown's method.[12] This synthetic

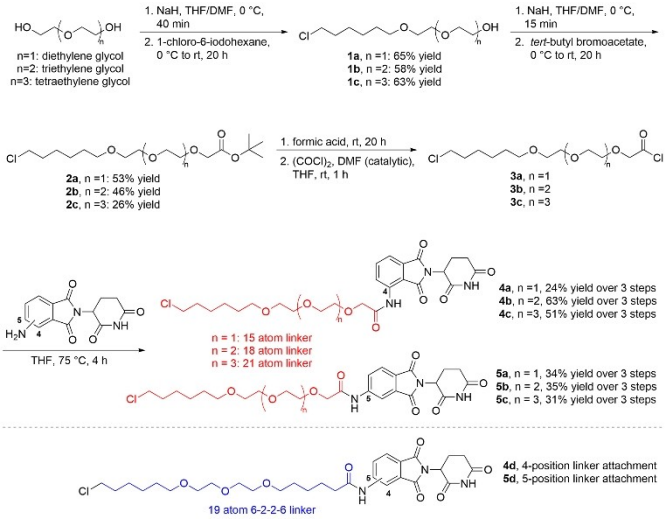

Scheme 1. Synthesis of CRBN-engaging HaloPROTACs.

sequence rapidly produced CRBN-recruiting HaloPROTACs **4a**–**4c** and **5a**–**5c** with the linker attached to the 4- or 5-position of CRBN in yields of 24–63% over the three-step sequence. The linker length in these HaloPROTACs varies between 15 and 21 atoms between the chlorine atom and the nitrogen attachment point to the thalidomide core. Using similar chemistry, we also prepared HaloPROTACs **4d** and **5d** with a 19-atom linker shown in Scheme 1 using the commonly employed 6-2-2-6 PROTAC linker developed by Crews.[13] As shown in Scheme S1, these HaloPROTACs were prepared in yields of 68% and 52% over a three-step sequence starting from the 6-2-2-6 linker containing the *tert*-butyl ester.

With our targeted library of eight novel CRBN-pairing HaloPROTACs in hand, we studied their ability to degrade HaloTagged EGFP in HEK293 cells following a previous report

on the development of HaloPROTAC-3.[4d] We first transfected the cells with the EGFP-HaloTag2 expression plasmid to induce its expression and then treated the cells with varying concentrations of the HaloPROTAC compounds ranging from 0.001 to 2 μM. After overnight incubation of the compounds with the cells, we measured the extent of EGFP degradation by fluorescence imaging of the cells and by western blotting of the cell lysates probed with an anti-EGFP antibody.

As shown in Figure 2A, all HaloPROTACs with the linker anchored at the 4-position of the CRBN ligand degraded ≥80% of the EGFP-HaloTag2 fusion at 1 μM except **4d**. **4b** was particularly potent, degrading more than 80% of the EGFP-HaloTag2 at 10 nM. These results demonstrated the overall suitability of the pomalidomide core for HaloPROTAC development and revealed some interesting trends. First, in the 4-position linker series, **4b** with an 18-atom linker was the most potent degrader with an estimated half-maximal degradation concentration (DC_{50}) of 0.46 nM (Figure S1A). **4c** with one additional ethylene glycol unit in the 21-atom linker was less potent compared to **4b**, but still achieved close to 80% degradation of EGFP-HaloTag2 at 100 nM concentration of the compound. In contrast, **4a** with a 15-atom linker of one ethylene glycol unit shorter than **4b** was less active than **4b** and **4c** at 100 nM concentration (60% of EGFP-HaloTag2 degradation). These results suggest that the 18-atom linker in **4b** is the optimal length in the 4-position linker series for inducing degradation of the EGFP-HaloTag2 fusion. Secondly, in addition to linker length, the linker composition also affected degradation. HaloPROTAC **4d** has a 19-atom linker with a 6-2-2-6 assembly that consists of two ethylene glycol units in the middle flanked by two 6 carbon units. The large decrease in **4d**'s activity (less than 50% of EGFP-HaloTag2 degradation at

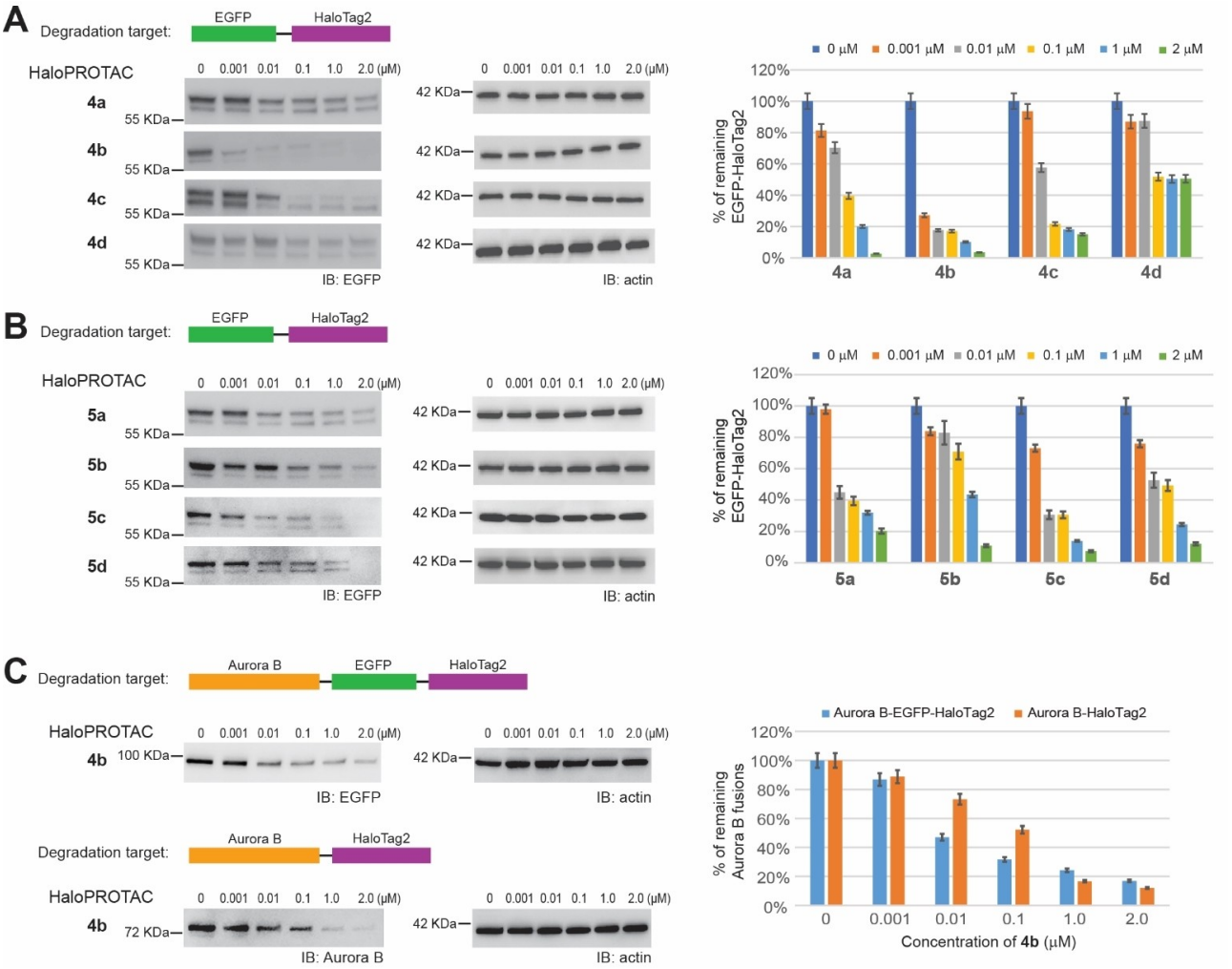

Figure 2. Activities of CRBN-targeting HaloPROTAC in inducing the degradation of EGFP-HaloTag2 fusion in HEK293 cells. Activities of **4a**–**4d** and **5a**–**5d** in degrading HaloTagged EGFP are shown in (A) and (B), respectively. Cells expressing HaloTagged EGFP were treated with the HaloPROTAC compounds for overnight at increasing concentrations. The level of EGFP-HaloTag2 in the cell was assayed by western blotting of the cell lysate probed with an anti-EGFP antibody. The western blots of the cell lysate were also probed with an anti-actin antibody as a loading control. Quantitative analyses of EGFP-HaoTag2 level in the cell lysates, as shown by the western blots, were plotted in the bar chart on the right. The vertical bars in the chart represent SEM from three independent experiments (n = 3). (C) Degradation of Aurora B-EGFP-HaloTag2 fusion (upper panels) and Aurora B-HaloTag2 fusion (lower panels) in HEK293 cells treated with compound **4b**. The levels of the fusion protein in the cell lysates were probed with an anti-EGFP or anti-Aurora B antibody and plotted in the chart on the right. The band intensity of the HaloTag2 tagged proteins was normalized to the actin control for comparing protein degradation in all the bar charts.

100 nM of **4d**) suggests that the increased aliphatic character of the linker affects the degradation efficiency. In addition to western blotting, we also imaged the fluorescence from cells expressing EGFP and found fewer cells with intense EGFP fluorescence after treating the cells with increasing concentration of HaloPROTACs of this series (Figure S2A). These results corroborate the western blot assays demonstrating the activity of CRBN-engaging HaloPROTACs in inducing the degradation of Halotagged EGFP as the target protein.

For HaloPROTACs with the linker at the 5-position, **5c** with a 21-atom linker is the most potent as it achieves more than 80% degradation of EFGP-HaloTag2 at 1 μM and has an estimated DC_{50} value of 2.8 nM (Figure S1B). In contrast, **5a** and **5b** containing shorter linkers were less active, yielding around 60% degradation of EFGP-HaloTag2 at 1 μM of the compounds (Figure 2B). Interestingly, **5d** containing the 19-atom 6-2-2-6 linker structure displayed increased degradation over **4d** as it degraded ~80% of EFGP-HaloTag2 at 1 μM, demonstrating that the 5-postion attachment point tolerates increased aliphatic character in the linker. Cell imaging studies for the 5-position series also showed that increasing the concentration of HaloPROTACs with a 5-positioned linker led to a lower number of cells with EGFP fluorescence (Figure S2B).

When comparing the 4- and 5-postion series, the best compound in the 4-series, **4b**, was more active than the best compound in the 5-series, **5c**. This was especially apparent when low compound concentration was used to induce protein degradation – at 1 nM, **4b** achieved more than 70% degradation of EGFP-HaloTag2, while **5c** achieved a degradation of less than 30%. Importantly, we also found both series of CRBN-recruiting compounds were tolerated by the HEK293 cells as no significant cell death was observed in an MTT assay after treating HEK293 cells overnight with concentrations of **4b** and **5c** up to 10 μM (Figure S3). This demonstrated that the protein degradation induced by treatment with HaloPROTACs **4b** and **5c** at increasing concentrations was not due to these compounds inducing cell death.

For comparing the CRBN and VHL-engaging HaloPROTACs in parallel, we synthesized HaloPROTAC-3 (Figures 1 and 3) that was previously developed as the degraders of HaloTagged proteins by pairing with the VHL E3.[4d] We found HaloPROTAC-3 can efficiently degrade EGFP-HaloTag2 fusion with a DC_{50} value of 3.4 nM. The original report measured HaloPROTAC-3 activity in inducing the degradation of EGFP-HaloTag7 and reported a DC_{50} of 19 nM.[4d] By comparison, CRBN-pairing degrader **4b** from this study matches the efficiency of HaloPROTAC-3, and since **4b** has a DC_{50} value of 0.46 nM, it is more effective in inducing the degradation of EGFP-HaloTag2 at low compound concentrations. After treating the cell with 10 nM of the compounds, we found **4b** induced close to 80% degradation of EGFP fusion while HaloPROTAC-3 induced about 60% degradation (Figure 3).

To demonstrate the activity of **4b** in inducing the degradation of mammalian proteins, we constructed an expression plasmid of Aurora B kinase with C-terminal tags of EGFP-HaloTag2 and expressed the fusion protein in HEK293 cells. We found **4b** could degrade 50% of the Aurora B fusion at a concentration as low as 10 nM and that ~80% degradation was achieved with a concentration of 1 μM (Figure 2C and S4). A time course experiment of the degradation assay with 10 nM of **4b** suggests a significant degradation of AuroraB-EGFP-HaloTag2 within 12 hours (Figure 4A). Furthermore, treatment of the cell with proteasome inhibitor MG132 decreased the degradation of the fusion protein induced by **4b** (Figure 4B), suggesting that the proteasome mediates the degradation of the protein targeted by the pomalidomide-based HaloPROTACs. In another experiment, we expressed Aurora B-HaloTag2 fusion protein

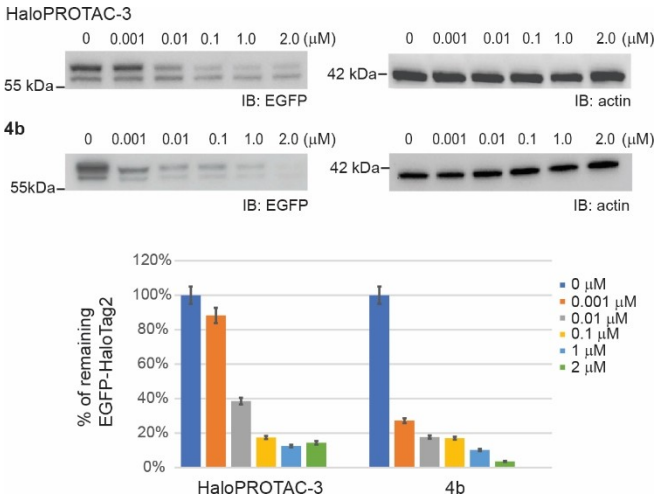

Figure 3. Comparison of activities of VHL-recruiting HaloPROTAC-3 in inducing the degradation of EGFP-HaloTag2 fusion in HEK293 cells. Cells expressing HaloTagged EGFP were treated with HaloProtac-3 or **4b** for overnight at increasing concentrations. The level of EGFP-HaloTag2 fusion in the cell was assayed by western blotting of the cell lysate probed with an anti-EGFP antibody. The level of actin in the cell lysate was also measured by western blotting as a loading control. Quantitative analyses of the levels of EGFP-HaoTag2 in the cell lysates were carried out by measuring the band intensities on the western blots, and the data were plotted in the bar chart. The vertical bars in the chart represent SEM from three independent experiments (n = 3). The band intensity of EGFP-HaloTag2 was normalized to the actin control for comparing protein degradation in the bar charts.

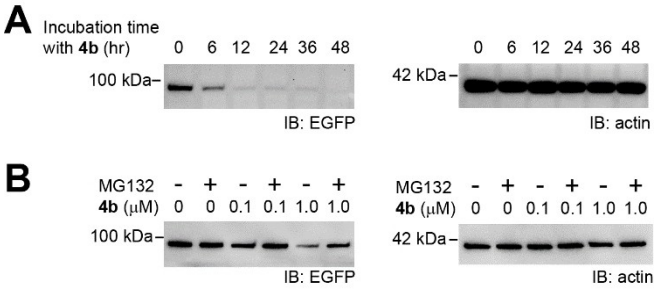

Figure 4. Degradation of Aurora B-EGFP-HaloTag2 fusion by **4b**. (A) Time course assay for the degradation of Aurora B-EGFP-HaloTag2 by **4b**. Cells expressing the fusion protein were treated with 10 nM of **4b** for 6, 12, 24, 36, and 48 hours and the amount of the fusion protein in the cell was assayed by western blot probed with an anti-EGFP antibody. (B) Effects of proteosome inhibitor MG132 on the degradation of AuroraB-EGFP-HaloTag2 fusion induced by **4b**. Cells expressing the fusion protein was co-treated with 10 μm MG132 and 0.1 or 1 μM **4b** for 4 hours. The fusion protein levels in the cell were assayed by western blot probed with an anti-EGFP antibody.

without EGFP in HEK293 cells and treated the cells with varying concentrations of **4b**. We found **4b** can degrade Aurora B-HaloTag2 fusion with a similar efficiency for degrading Aurora B-EGFP-HaloTag2 fusion at concentrations greater than 1 μM (Figure 2C).

In conclusion, in this study, we developed HaloPROTACs that can utilize the CRBN E3 for degrading HaloTagged proteins and demonstrate the matching efficiency of the CRBN-recruiting ligands with the VHL-recruiting ligands in inducing degradation of HaloTagged EGFP as a model target. By varying the linker length and position of attachment to the pomalidomide core, we identified compound **4b** equipped with an 18-atom/3-PEG unit linker anchored at the 4-position of pomalidomide as the most efficient degrader ($DC_{50} = 0.46$ nM), and it exceeds the efficiency of VHL-pairing HaloPROTAC-3 in inducing the degradation of HaloTagged EGFP at sub-micromolar concentrations of the compounds. We expect the CRBN-pairing **4b** can be broadly applied to target validation for PROTACS similarly to its VHL-pairing counterparts.

Besides the HaloPROTAC system, a variety of platforms for validating PROTAC targets have been developed, with the HaloPROTAC and dTAG systems being most broadly used. The lack of a CRBN compatible HaloPROTAC stands in contrast to the dTAG system that has ligands to promote degradation through both VHL and CRBN.[5] The development of CRBN-engaging HaloPROTACs in this study provides a useful complement to the VHL-engaging HaloPROTACs and would expand the target validation platform for PROTAC development based on HaloTag fusions. The strength of the HaloTag platform stems from its generalizability to a variety of applications, including protein isolation and purification and the study of protein localization, function, and interactions. The commercial availability of 20,000 HaloTag-protein fusion proteins[4d] and the demonstrated ability to use CRISPR/Cas9 genome editing to generate HaloTag fusion proteins for endogenous proteins[4a,14] makes the HaloPROTAC platform applicable for investigating a wide range of potential therapeutic targets. The further extension of this readily available platform to targeted protein degradation amplifies the value of this technology as the installation of the HaloTag can be leveraged consecutively to study protein localization, interactions, and degradation.[15] The discovery of HaloPROTACs that engage the CRBN E3 ligase extends the versatility of the HaloTag/HaloPROTAC system for target exploration and validation through ubiquitination pathways mediated by various E3s.

Experimental Section

Details of the experimental procedures are provided in the Supporting Information.

Author Contributions

M. T. and J. Y. conceived the ideas and designed the HaloPROTAC ligands. B. K. O. synthesized HaloPROTAC ligands **5a**–**c** and intermediate S2, optimized the degradation assay based on fluorescence imaging, assayed the activity of the ligands, established the degradation ability of the CRBN haloPROTACs, and provided data for Figures S2, S3 and S4. J.Z. and Y.X. assayed the activity of the ligands and provided the data for Figures 2, 3, 4, S1, and S2. S. E. N. designed the HaloPROTAC synthesis, synthesized HaloPROTAC ligands **4a**–**d** and **5d**, and assisted with the degradation assays. R. L. optimized the degradation assay based on western blotting. C. J. D. synthesized HaloPROTAC-3. S. E. J. cloned Aurora B expression plasmid. S. L. W. and L. A. W. assisted ligand synthesis B. K. O., J. Z., S. E. N., Y. X., S. G., M. T., and J. Y. analyzed data and interpreted results. J. Y. and M. T. drafted and edited the manuscript. All authors reviewed and approved the final version of the manuscript.

Acknowledgements

This work was supported by NSF (1710460 and 2109051 to J. Y.) and NIH (R01GM104498 to J. Y.). S. E. N. gratefully acknowledges support from the Berry College Synovus and Richards Scholars Program. R. L. is supported by the Molecular Basis of Disease (MBD) program of Georgia State University.

Conflict of Interests

The authors declare no conflict of interest.

Data Availability Statement

The data that support the findings of this study are available in the supplementary material of this article.

Keywords: PROTAC · HaloTag · HaloPROTAC · ubiquitin · Cereblon

[1] a) J. Lu, Y. Qian, M. Altieri, H. Dong, J. Wang, K. Raina, J. Hines, J. D. Winkler, A. P. Crew, K. Coleman, C. M. Crews, *Chem. Biol.* **2015**, *22*, 755–763; b) D. P. Bondeson, A. Mares, I. E. Smith, E. Ko, S. Campos, A. H. Miah, K. E. Mulholland, N. Routly, D. L. Buckley, J. L. Gustafson, N. Zinn, P. Grandi, S. Shimamura, G. Bergamini, M. Faelth-Savitski, M. Bantscheff, C. Cox, D. A. Gordon, R. R. Willard, J. J. Flanagan, L. N. Casillas, B. J. Votta, W. den Besten, K. Famm, L. Kruidenier, P. S. Carter, J. D. Harling, I. Churcher, C. M. Crews, *Nat. Chem. Biol.* **2015**, *11*, 611–617; c) A. C. Lai, C. M. Crews, *Nat. Rev. Drug Discovery* **2017**, *16*, 101–114; d) K. M. Sakamoto, K. B. Kim, A. Kumagai, F. Mercurio, C. M. Crews, R. J. Deshaies, *Proc. Natl. Acad. Sci. USA* **2001**, *98*, 8554–8559.

[2] a) D. P. Bondeson, C. M. Crews, *Annu. Rev. Pharmacol. Toxicol.* **2017**, *57*, 107–123; b) G. M. Burslem, C. M. Crews, *Chem. Rev.* **2017**, *117*, 11269–11301; c) M. S. Gadd, A. Testa, X. Lucas, K. H. Chan, W. Chen, D. J. Lamont, M. Zengerle, A. Ciulli, *Nat. Chem. Biol.* **2017**, *13*, 514–521.

[3] a) M. Zengerle, K. H. Chan, A. Ciulli, *ACS Chem. Biol.* **2015**, *10*, 1770–1777; b) Y. Itoh, M. Ishikawa, M. Naito, Y. Hashimoto, *J. Am. Chem. Soc.* **2010**, *132*, 5820–5826.

[4] a) H. Tovell, A. Testa, C. Maniaci, H. Zhou, A. R. Prescott, T. Macartney, A. Ciulli, D. R. Alessi, *ACS Chem. Biol.* **2019**, *14*, 882–892; b) L. M. Simpson, T. J. Macartney, A. Nardin, L. J. Fulcher, S. Roth, A. Testa, C. Maniaci, A. Ciulli, I. G. Ganley, G. P. Sapkota, *Cell Chem. Biol.* **2020**, *27*, 1164–1180;

c) T. K. Neklesa, H. S. Tae, A. R. Schneekloth, M. J. Stulberg, T. W. Corson, T. B. Sundberg, K. Raina, S. A. Holley, C. M. Crews, *Nat. Chem. Biol.* **2011**, *7*, 538–543; d) D. L. Buckley, K. Raina, N. Darricarrere, J. Hines, J. L. Gustafson, I. E. Smith, A. H. Miah, J. D. Harling, C. M. Crews, *ACS Chem. Biol.* **2015**, *10*, 1831–1837.

[5] a) B. Nabet, F. M. Ferguson, B. K. A. Seong, M. Kuljanin, A. L. Leggett, M. L. Mohardt, A. Robichaud, A. S. Conway, D. L. Buckley, J. D. Mancias, J. E. Bradner, K. Stegmaier, N. S. Gray, *Nat. Commun.* **2020**, *11*, 4687; b) B. Nabet, J. M. Roberts, D. L. Buckley, J. Paulk, S. Dastjerdi, A. Yang, A. L. Leggett, M. A. Erb, M. A. Lawlor, A. Souza, T. G. Scott, S. Vittori, J. A. Perry, J. Qi, G. E. Winter, K. K. Wong, N. S. Gray, J. E. Bradner, *Nat. Chem. Biol.* **2018**, *14*, 431–441.

[6] A. G. Bond, C. Craigon, K. H. Chan, A. Testa, A. Karapetsas, R. Fasimoye, T. Macartney, J. J. Blow, D. R. Alessi, A. Ciulli, *J. Med. Chem.* **2021**, *64*, 15477–15502.

[7] C. Grohmann, C. M. Magtoto, J. R. Walker, N. K. Chua, A. Gabrielyan, M. Hall, S. A. Cobbold, S. Mieruszynski, M. Brzozowski, D. S. Simpson, H. Dong, B. Dorizzi, A. V. Jacobsen, E. Morrish, N. Silke, J. M. Murphy, J. K. Heath, A. Testa, C. Maniaci, A. Ciulli, G. Lessene, J. Silke, R. Feltham, *Nat. Commun.* **2022**, *13*, 2073.

[8] C. G. England, H. Luo, W. Cai, *Bioconjugate Chem.* **2015**, *26*, 975–986.

[9] a) S. Tomoshige, M. Naito, Y. Hashimoto, M. Ishikawa, *Org. Biomol. Chem.* **2015**, *13*, 9746–9750; b) S. Tomoshige, Y. Hashimoto, M. Ishikawa, *Bioorg. Med. Chem.* **2016**, *24*, 3144–3148.

[10] M. Schapira, M. F. Calabrese, A. N. Bullock, C. M. Crews, *Nat. Rev. Drug Discovery* **2019**, *18*, 949–963.

[11] H. S. Tae, T. B. Sundberg, T. K. Neklesa, D. J. Noblin, J. L. Gustafson, A. G. Roth, K. Raina, C. M. Crews, *ChemBioChem* **2012**, *13*, 538–541.

[12] S. M. Capitosti, T. P. Hansen, M. L. Brown, *Org. Lett.* **2003**, *5*, 2865–2867.

[13] A. C. Lai, M. Toure, D. Hellerschmied, J. Salami, S. Jaime-Figueroa, E. Ko, J. Hines, C. M. Crews, *Angew. Chem. Int. Ed. Engl.* **2016**, *55*, 807–810.

[14] E. A. Caine, S. D. Mahan, R. L. Johnson, A. N. Nieman, N. Lam, C. R. Warren, K. M. Riching, M. Urh, D. L. Daniels, *Curr Protoc Pharmacol* **2020**, *91*, e81.

[15] D. Zhao, Z. Yin, M. B. Soellner, B. R. Martin, *Cell Chem. Biol.* **2021**, *28*, 1235–1241.

Manuscript received: July 6, 2023
Revised manuscript received: August 24, 2023
Accepted manuscript online: August 25, 2023
Version of record online: September 13, 2023